International Journal of Heat and Technology
Vol. 44, No. 1, February, 2026, pp. 45-58
Journal homepage: http://iieta.org/journals/ijht

Numerical Analysis of Mixed Convection in Vented Triangular Cavity with Bottom-Mounted Adiabatic Fin

Huda Abdullah Al-Mayahi[1], Zuhal AbdulHadi Hamza[2], Wisam S. Hacham[3*], Sana J. Yaseen[1]

[1] Mechanical Engineering Department, University of Basrah, Basrah 61004, Iraq
[2] Department of Civil Engineering, University of Basrah, Basrah 61004, Iraq
[3] Mechatronics Engineering Department, Al-Khwarizmi College of Engineering, University of Baghdad, Baghdad 10071, Iraq

Corresponding Author Email: wisam@kecbu.uobaghdad.edu.iq

Copyright: ©2026 The authors. This article is published by IIETA and is licensed under the CC BY 4.0 license (http://creativecommons.org/licenses/by/4.0/).

https://doi.org/10.18280/ijht.440105

Received: 7 October 2025
Revised: 13 January 2026
Accepted: 27 January 2026
Available online: 28 February 2026

Keywords:
fin optimization, heat transfer enhancement, laminar flow, mixed convection, triangle cavity

ABSTRACT

Mixed convective heat transfer has a critical impact on improving thermal performance of many engineering components, like cooling apparatus and heat exchangers. While either experiments supported by numerical solution studies or through practical experiments separate from numerical solutions have diversely examined this phenomenon in copious geometries, an effect of expanding the effective flow area—with non-uniform boundary conditions—on the thermal performance is not fully covered, to the authors' knowledge. This study numerically investigates mixed convective heat transfer in a vented triangular cavity with a thermally insulating fin on the bottom warm wall, to contribute to fill this gap. The cavity features a cold left wall, a thermally insulating right wall, and open vent areas for incoming (bottom left) and outgoing (top right) fluid flow. Using Flex Partial Differential Equations (FlexPDE) software, the analysis examines—utilizing water (Prandtl Number: Pr = 7) as the working fluid—the effects of key parameters, such as fin length ($0.1 \leq L_f \leq 0.3$), fin position ($0.4 \leq h \leq 0.8$), Richardson number ($0.1 \leq Ri \leq 10$), and Reynolds number ($50 \leq Re \leq 100$). The results show that the average Nusselt number (Nu_{avg}) increases with changing fin position from 0.4 to 0.8 by 6.75 % due to the increased convective flow along the heated surface, where optimal fin placement is 0.8, which improves thermal performance by expanding the effective flow area. These results form a novel model to this work and include the threefold: the distinctive and adiabatic triangular vented cavity geometry with adiabatic fin on the hot wall; adiabatic fin use merely as a flow control technique, to increase the effective flow area; and a systematic parametric study of the positioning and length of the fins in a mixed convection regime, never before revised in the literature as applied to this particular geometry.

1. INTRODUCTION

Convective heat transfer and fluid flow within enclosure areas have always been of interest to scholars, due to the subject's widespread nature. There are three types of convection, and they are: natural convection, this is caused by buoyant forces due to a difference in density connected to temperature differentials Ri < 0.1 the second type is forced convection which occurs when an external source such as a pump or fan is utilized to produce convection $Ri > 10$, and the last convection is combined convection which is mixed between natural and forced $0.1 \leq Ri \leq 10$. Applications for the convective heat transport are numerous, cooling of electronics equipment [1-5], solar collectors [6, 7], heat exchangers [8, 9], etc.

The effect of an inclined baffle on free convective in a container containing two different nanofluids (Al_2O_3-H_2O and Cu-H_2O) was investigated by AL-Farhany et al. [10, 11]. The right side was cool, the left side thick and hot, and the other side adiabatic. When the hot wall's thickness increases, the result is less heat transfer. The stream function reached its peak when the baffle's angle equaled 60. Experimental free convective was examined by Al-Maliki et al. [12] in a rectangular container that held a hybrid nanofluid. Phase Change Material (PCM) was fixed to a heated wall; the other walls were adiabatic, and the wall opposite it was cold. Consequently, it was found that the PCM could potentially reduce the hot wall's temperature by up to 22%. The examination of the effect of Magnetohydrodynamics (MHD) in a porous enclosure with two fins was investigated by Al-Farhany et al. [13] and Canazas and Kamyshnikov [14]. Mixed convection was examined by Velkennedy et al. [15] in an open rectangular enclosure. The upper wall is where the fins are fastened. While the other walls were heated, the lower wall was adiabatic. There was a working fluid used, air. The outcome showed that increased buoyancy force improves heat transport. Additionally, Selimefendigil and Chamkha [16] investigated the effects of MHD in three-dimensional open enclosures. Alhussain [17] investigated mixed convection in a square chamber with multiple ventilation ports. The effect of a magnetic field on mixed convective flow in a vented cavity was investigated by Shaker et al. [18]. Reynolds number (200

≤ Re ≤ 600) and magnetic number ($0 \leq Mn \leq 5 \times 10^7$) are two examples of the influencing factors. Many studies on mixed convection with fins or baffles in various open cavities or channels have been conducted recently [19-24].

Although models mentioned above have different designs and arrangements, they tried to improve thermal efficiency, each according to its research philosophy. Many of them has demonstrated that there are significantly enhances in heat transfer performance due to expanding the effective flow area. In any case, the optimal design remains open to all possibilities in many real-world models, like in advanced microprocessors, where the heating is essentially non-uniform, introducing complex flow patterns and localized thermal stresses not accurately predicted by most current models. Efficient design and model argument for increasing thermal performance—by expanding the effective flow area—remains inadequately explored.

While fundamental studies of mixed convection in enclosures are abundant, the triangular vented cavity with a bottom-mounted adiabatic fin examined in this work addresses specific, practical thermal management challenges in modern engineering. This configuration is particularly relevant to compact and non-standard heat exchangers, advanced electronics cooling (e.g., GPU/CPU corner cooling), solar thermal collector channels, and architectural ventilation of attic-like spaces.

In aerospace, automotive, and portable electronics, spatial constraints often necessitate heat exchangers with irregular, non-rectangular flow passages to maximize surface area within limited volumes. Triangular or trapezoidal ducts are common in such compact designs [6, 8]. The present geometry serves as a fundamental unit to model flow and heat transfer in these corner-fitted modules.

High-power microelectronics, such as graphics processing units (GPUs) and multi-core processors, exhibit significant non-uniform, localized heating, often with peak temperatures near die corners. A triangular cavity segment can model a high-heat-flux corner region of a chip under a heatsink [3]. The adiabatic fin acts as a passive flow guide or "thermal boundary layer disruptor," redirecting coolant (e.g., water or dielectric fluid) to hotspot areas without adding conductive material that could create thermal stresses or short-circuiting risks—a key concern in 3D integrated circuits [25].

Certain designs of solar air heaters and photovoltaic-thermal (PV-T) systems employ triangular duct geometries to optimize absorber area and flow dynamics [7, 9]. An adiabatic fin attached to the heated absorber plate can function to break the laminar sublayer and enhance fluid mixing, thereby improving thermal efficiency without the parasitic heat loss associated with conductive extended surfaces [10].

The model is similar to natural or hybrid ventilation of attic spaces, A-frame buildings, or triangular pieces of the roof [17]. Here, the adiabatic fin is an element of structure or a strategically situated baffle designed to maximize air circulation, remove stagnant areas, and increase convective cooling of the occupied cavity.

The findings of the numerical research provide immediate design knowledge on thermal management of geometries with constraints. The main practical implication of this is that a strategically positioned adiabatic fin can act as a simple, cost-effective, and passive device, used to improve convective cooling by optimizing the field of flow. Specifically, for the case of electronics thermal designers, a flow-modifying feature (e.g., polymer rib or an insulated deflector) placed close to the trailing edge of an electronics chip heated surface (equivalent to an optimum position of h = 0.8) can enhance the convective heat transfer coefficient as shown by the 6.75% increase in Nu_{avg}. This can be employed in any case to reduce hot spots at corners in sophisticated packages [3, 5].

Without a comprehensive understanding of the effect on all designs, parameters, factors, and variables, the full understanding of thermal performance enhancement cannot be realized in groundbreaking thermal management systems, delaying the development of next-generation heat exchanger designs. To support current development scenarios, this study aims to numerically investigate mixed convective heat transfer in a vented triangular cavity with a thermally insulating fin on the bottom warm wall. Our analysis will clarify how expanding the effective flow area improves thermal performance, thereby presenting significant insights for enhancing cooling systems.

The systematic innovation gaps can be summarized as follows:

Geometry Gap: While numerous studies exist on square, rectangular, or complex 3D vented cavities, the mixed convection heat transfer in a simple 2D vented triangular cavity remains significantly under explored.

Function Gap: Most prior work on fins/baffles focuses on their role as: Conductive extenders (to increase surface area), or Active flow disrupters (e.g., rotating, flexible). The current study investigates a fin in a fundamentally different role: as a static, adiabatic flow moderator whose sole purpose is to strategically expand the effective flow area near the heated wall, thereby enhancing convective transport without adding conductive paths.

Parameter Interaction Gap: Previous studies often vary parameters like Ri, Re, or fin size in isolation within standard geometries. There is a lack of a systematic, coupled parametric study investigating the interaction between fin position (h), fin length (L_f), Re, and Ri, specifically within the unique flow domain of a vented triangle. Our work quantifies how optimal fin placement (e.g., h = 0.8) emerges from this interaction to maximize Nu_{avg}.

Although convective heat transfer has been widely researched, past studies have not yet investigated the performance of a unique triangular vented cavity with an adiabatic fin on the hot wall. However, the adiabatic fin is conventionally employed to augment heat transfer by expanding the surface area; this paper only considers the adiabatic fin as a method of flow control to augment the effective flow jet. As a result, we developed a new approach to fin positioning and length in a mixed convection regime to offset this important gap in the literature. Therefore, the novelty of this work is not merely the sum of its parts, but in the conceptual combination and systematic interrogation of a passive adiabatic fin within a vented triangular cavity to elucidate the mechanism and optimization of "effective flow area expansion" for mixed convection enhancement—a gap not addressed by the existing literature.

2. METHODOLOGY

This study outlines a comprehensive approach to thermal analysis, encompassing the essential steps of problem definition and solution verification. We begin by detailing the physical model under consideration, followed by presenting the relevant governing equation. Next, the necessary boundary

conditions will be precisely defined, providing the constraints necessary for a satisfactory solution. These conditions are essential for accurately simulating real-world thermal reactions. The methodology then moves on to describe the numerical solutions used to solve the governing equation, taking into account the specified boundary conditions. Finally, the solution will be thoroughly validated to ensure the accuracy and reliability of the numerical results, often by comparing them with experimental data or validated analytical solutions.

2.1 Physical model

Figure 1 illustrates the two-dimensional (2D) triangle vented cavity. The bottom wall is heated (T_h), the right-hand side wall is adiabatic, and the left wall is cold (T_c). The fin thickness is assumed to be fixed at a constant value. The single fin is fixed to the hot wall at different lengths (L_f = 0.1, 0.2, and 0.3) and locations (h = 0.4, 0.6, and 0.8). Assuming an open area of (W_{in} = 0.1), the cold fluid input to the enclosure is equal to that of the upper side outlet area (W_{out} = 0.1). It is assumed that the fluid exits the cavity at atmospheric pressure, but it enters the cavity at a cold temperature (T_{in}). The working fluid selected is water at a Prandtl number (Pr) of 7.

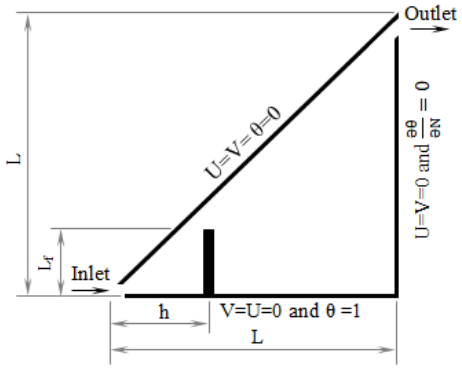

Figure 1. The two-dimensional (2D) pattern of a triangular vent cavity, containing the boundary conditions

2.2 The conservation equations

The dimensionless forms of governing equations for continuity, energy, and momentum are given by [10, 26-30]:

Continuity

$$\frac{\partial U}{\partial X}+\frac{\partial V}{\partial Y}=0 \tag{1}$$

Momentum

$$U\frac{\partial U}{\partial X}+V\frac{\partial U}{\partial Y}=-\frac{\partial P}{\partial X}+\frac{1}{R_e}\left(\frac{\partial^2 U}{\partial X^2}+\frac{\partial^2 U}{\partial Y^2}\right) \tag{2}$$

$$U\frac{\partial V}{\partial X}+V\frac{\partial V}{\partial Y}=-\frac{\partial P}{\partial Y}+\frac{1}{R_e}\left(\frac{\partial^2 V}{\partial X^2}+\frac{\partial^2 V}{\partial Y^2}\right)+R_i\theta \tag{3}$$

Energy

$$U\frac{\partial \theta}{\partial X}+V\frac{\partial \theta}{\partial Y}=\frac{1}{R_e P_r}\left(\frac{\partial^2 \theta}{\partial X^2}+\frac{\partial^2 \theta}{\partial Y^2}\right) \tag{4}$$

where, X, Y, U, V, θ, P^*, P_r, R_i (Richardson number), and G_r (Grashof number) are the dimensionless variables define as $\frac{x}{L}$, $\frac{y}{L}$, $\frac{u}{u_{in}}$, $\frac{v}{u_{in}}$, $\frac{T-T_{in}}{T_h-T_{in}}$, $\frac{p}{\rho u_{in}^2}$, $\frac{v}{\alpha}$, $\frac{G_r}{Re^2}$, and $\frac{g\beta(T_h-T_{in})L^3}{v^2}$, respectively, while ρ and u_{in} are the density and inlet velocity, respectively.

2.3 Boundary conditions

The mathematical expressions—translating the actual thermal responses into a solvable formula—that describe the heat flow at the edges of the considered domain. In the current study, the inlet boundary conditions are U = 1, V = 0, and θ = 0. At the bottom, inclined, and right walls of the studied enclosure, U and V equal 0, where θ = 1, θ = 0, and $\frac{\partial\theta}{\partial N}=0$ at the bottom, inclined, and right walls of the enclosure, respectively. The P^* at the outlet equals 0.

2.4 Numerical solutions

The governing Eqs. (1) to (4) and the related boundary conditions are numerically solved by Finite Element Methodology (FEM), using the software package Flex Partial Differential Equations (FlexPDE) [29]. The continuity equation must be applied as a constraint because of mass conservation, and the pressure distribution may be obtained by applying this constraint [30, 31]. Eqs. (2) to (4) can be solved using a penalty parameter and the compressibility criterion by Eq. (1), which results:

$$\nabla^2 P=\gamma\left(\frac{\partial U}{\partial X}+\frac{\partial V}{\partial Y}\right) \tag{5}$$

As a penalty parameter, γ should be found using physical knowledge or alternative techniques [24, 32, 33]. The study determined that the most practical value was ($10^{11}/L^2$). In terms of isotherms, U- and V-velocities, and velocity lines, the numerical solutions are derived. The bottom wall's average Nusselt number along the heated surface [34].

$$N_{u_{avg}}=\int_0^1\left(\frac{\partial\theta}{\partial y}\right)_{y=0}.dx \tag{6}$$

Also, the bulk temperature is calculated from the relation

$$\theta_{avg}=\int\frac{\theta d\bar{v}}{\bar{v}} \tag{7}$$

where, $\bar{v}$ is the volume of occupying fluid in the triangle cavity.

2.5 Validation

The continuity equation ($\partial u/\partial x + \partial v/\partial y$) = 0, and several grid size sensitivity tests were performed in Figure 2. This accuracy is compromised vale between the result accuracy and the time consumed in each run. The grid domain for Re = 50, Ri-0.1, h = 0.8, and L_f = 0.2. The findings demonstrated the exact validation of the velocity distribution for the grid size established by applying an accuracy of 10^{-3}. Figure 3 shows the validation with the previous work [24]. Mixed convection in a vented square cavity with a fixed fin on the left wall at Re = 50, Ri = 1, h = 0.8, and L_f = 0.4. The results are of a great quality. As a result, the confidence in the numerical solution is enhanced.

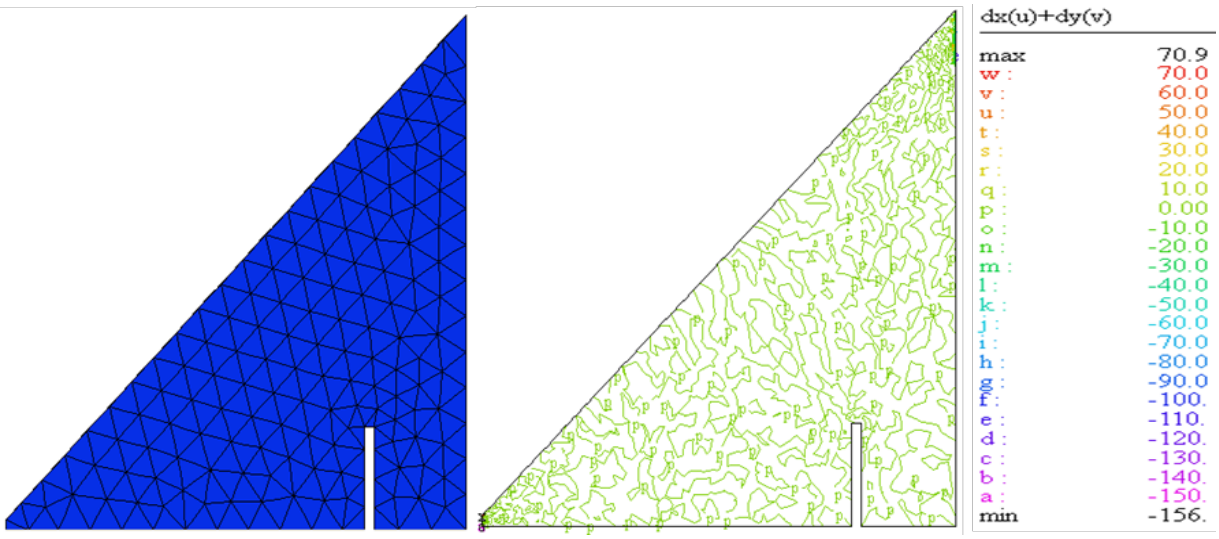

Figure 2. Grid generation distribution over the domain (left) and validity of continuity equation (right)

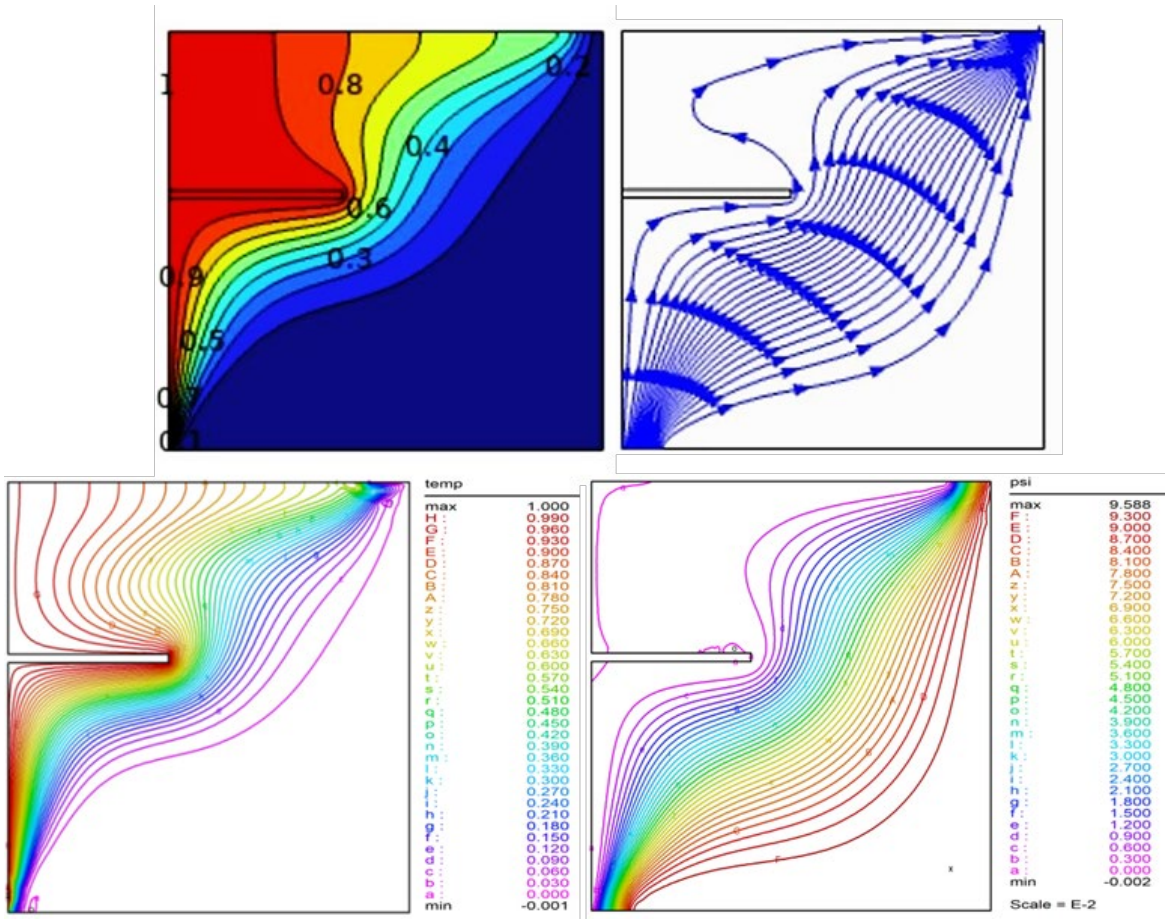

Figure 3. Velocity distribution of the previous work [24] (upper panel) and the current work (lower panel). The grid size is established by applying an accuracy of 10^{-3}

3. RESULTS AND DISCUSSIONS

This numerical analysis of mixed convection heat transfer focuses on a 2D cavity with a fin mounted on the bottom hot wall. At the bottom of the cavity, a cold fluid enters through the inlet (W_{in}) and exits at the top through the outlet (W_{out}). Using water (Pr = 7) as the working fluid for the analysis, the influence of dimensionless parameters on the flow field patterns, e.g., stream function (psi), thermal distribution, e.g., isotherms (θ), and heat transfer performance (e.g., mean Nusselt number Nu_{avg}) will be emphasized. The dimensionless parameters considered are the Reynolds number (Re), Richardson number (Ri), fin length (L_f), and fin position (h). The analysis results also provide insight into how the convective and mixed convection heat transfer behavior of the cavity changes with respect to these variables.

The following sub-sections will present the effect of fin position, fin length (L_f), Re number, and Ri number on

isotherms and streamlines (Ψ). Further, the effect of the Re number on Nu_{avg}. Furthermore, the effect of the Richardson number, fin position, and fin length on the Nusselt number.

3.1 Fin position (h) effect on isotherms and streamlines

For fixed values of Re = 50 and Ri = 0.1, the various locations (h = 0.4, 0.6, and 0.8) of a fin length (L_f = 0.2) are shown in Figure 4. The visualizing vortices—the primary vortex above the fin—are small to moderate, depending on the fin length (L_f), and cause flow separation when the cold fluid from the inlet hits the fin at h = 0.4. Clockwise rotation—as viewed from inside the cavity—combines the hot and cold fluids, improving local heat transfer. The small secondary vortex near the inlet causes the fin to deflect the cold fluid entering at the inlet downward. The angular vortex (i.e., top right, near the outlet) causes the hot, buoyant fluid rising along the inclined cold wall to meet the outgoing flow. This occurs frequently if natural convection is dominant. After passing the fin, the weak vortex along the inclined wall causes the flow to counterclockwise reconnect, leading to a weak circulation. At h = 0.6, it is observed that the vortex above the fin increases in size and extends a greater distance, approaching the vortex near the outlet. The two vortices on the inclined surface converge in size, resulting in increased fluid mixing and increased heat transfer. At h = 0.8, a large vortex is observed to form along the inclined surface, while the other vortices are more uniform along the gap.

On the right side, the effect of fin position (h) on the isotherms is shown. It can be seen that the flow passes from the lower left corner of the domain to the upper right corner due to the inlet and outlet configuration. The fins cause recirculation zones and act as an obstacle to the flow. The fin positions influence the thermal mechanisms. At h = 0.4, the fin mass density increases, creating hot/cold zones. At h = 0.6, the fins divide the flow evenly, featuring balanced flow splitting and equal spacing between isotherms, enhancing heat transfer. At h = 0.8, the fluid moves around the fins, indicating strong recirculation of the fluid, indicating low thermal resistance and strong connection with isotherms concentrated near the fin.

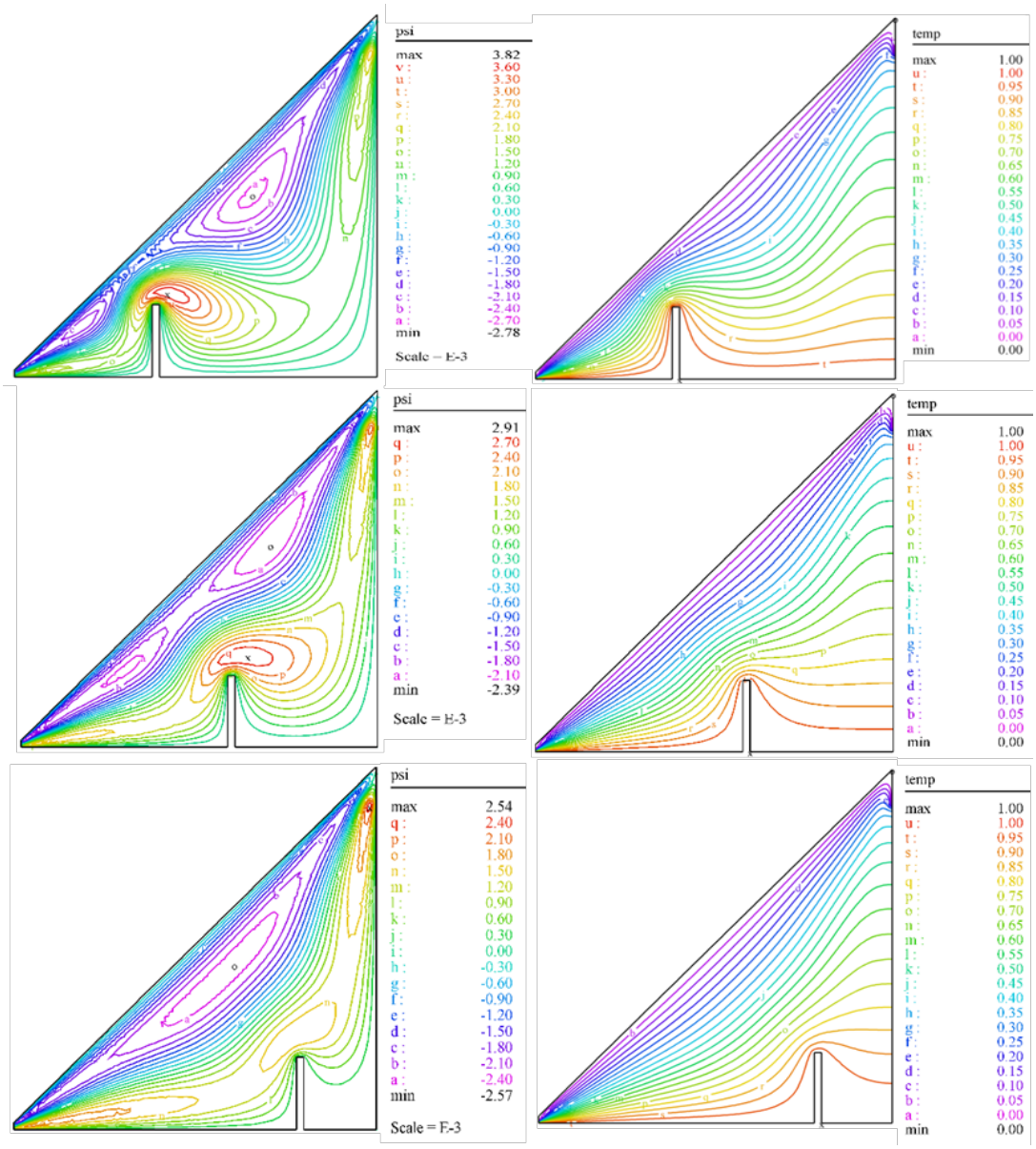

Figure 4. Streamlines (left) and isotherms (right) when L_f, Re, and Ri are 0.2, 50, and 0.1, respectively, and h equals 0.4 (upper), 0.6 (middle), and 0.8 (lower)

3.2 Effect of fin length (L_f) on isotherms and streamlines

Different flow regimes are demonstrated on the streamline patterns for different fin lengths (L_f), as shown in Figure 5. For a short fin (L_f = 0.1), there is little obstruction to the flow, which means only very weak recirculation very close to the fin, and other streamlines remain more or less undisturbed around the obstruction. As the fin becomes longer (L_f = 0.2) and becomes the predominant obstruction and block, there is more blockage in the flow, producing sizeable stagnant regions and larger recirculating zones behind the fin. When L_f = 0.3, it's observed that the effects of this blockage are most pronounced, as a recirculating zone with dominant flow was generated, which occupies a large portion of the volume in the cavity, pushing fluid to flow diverted around the fin close to the top wall and restricting the effective flow passage significantly.

The isotherm pattern in the right column shows that the shorter fin (L_f = 0.1) traced a relatively smooth, slightly turbulent isotherm, exhibiting the strongest convective and conductive heat transfer effects, with intermediate temperature gradients observed in the downstream isotherms. At L_f = 0.2, it produced a less smooth isotherm, forming a convergent, compressed isotherm around the fin. However, this can also be considered representative of the effect of recirculation on the redistribution of thermal energy, as indicated by the upward-curving shape of the downstream isotherms. The larger fin (L_f = 0.3) produced a strongly distorted isotherm due to compression at and around the fin base and ultimately a non-uniform isotherm influenced by recirculation effects. However, at the fin base, flow stagnation occurs, trapping thermal energy and reducing downstream heat transfer efficiency.

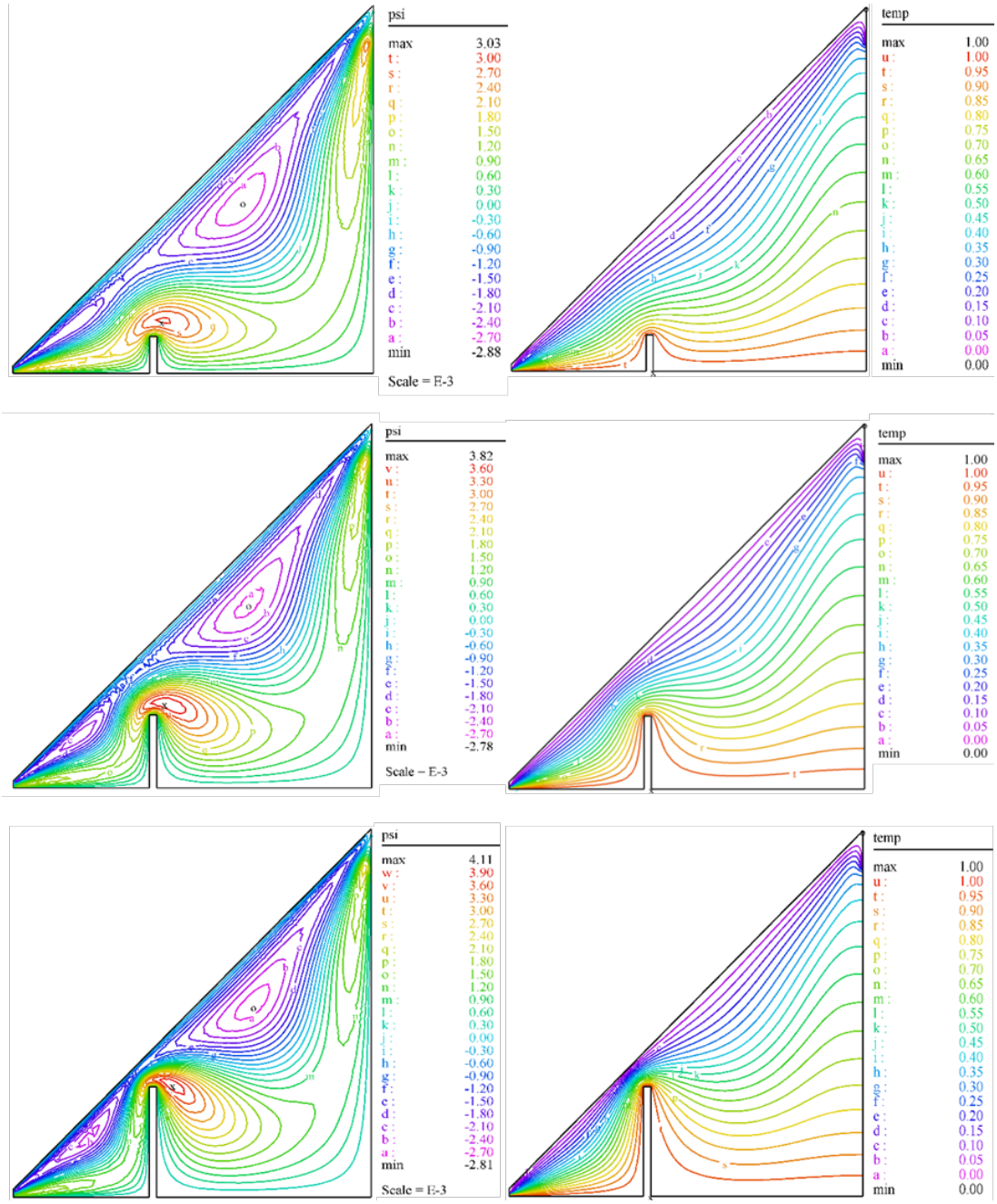

Figure 5. Streamlines (left) and isotherms (right) when h, Re, and Ri are 0.4, 50, and 0.1, respectively, and L_f equals 0.1 (upper), 0.2 (middle), and 0.3 (lower)

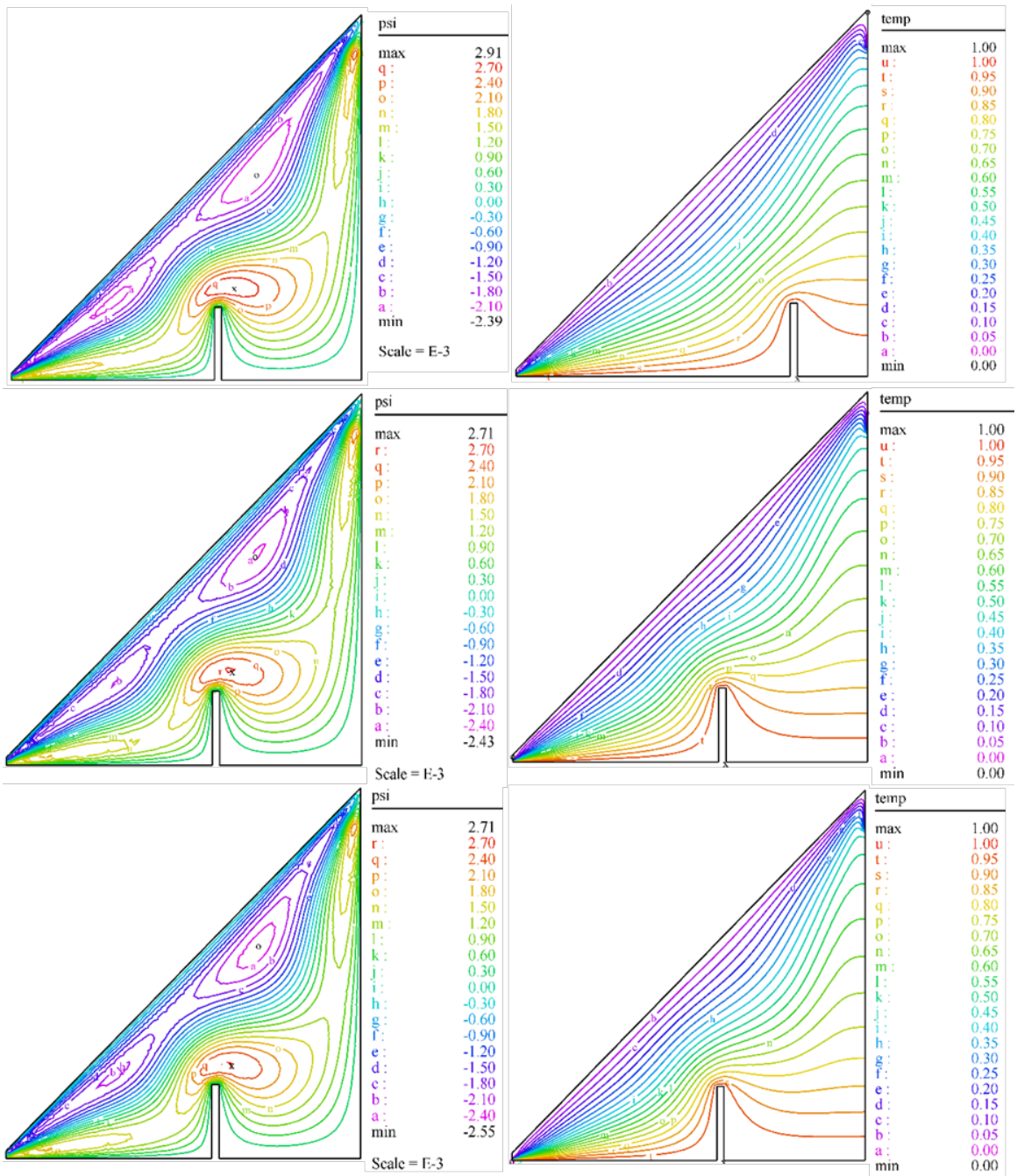

Figure 6. Streamlines (left) and isotherms (right) when L_f, h, and Ri are 0.2, 0.6, and 0.1, respectively, and Re equals 50 (upper), 80 (middle), and 100 (lower)

3.3 Re effect on isotherms and streamlines

The effect of the Re number on streamlines that are located at the left and isotherms at the right can be shown in Figure 6. This figure is plotted at constant values of L_f = 0.2, h = 0.6, and Ri = 0.1 for variable values of Re. There are four vortices in the cavity: Two located near the inclined wall and a small secondary vortex in the upper right corner of the cavity. The most intense vorticity occurs above the fin at all Re numbers. The vortex above the fin is affected by increasing Reynolds number, as its expansion increases with increasing Re number. The right column shows the isotherms at varying values of Re. At Re = 50, the isotherms are smooth, with nearly parallel isotherms, with slight distortion near the fin tip. As Re increases from 80 to 100, a pronounced curvature appears near the fin; the isotherms in the upper cavity are compressed and exhibit severe distortion near the fin.

3.4 Ri effect on isotherms and streamlines

Figure 7 shows the effect of the Richardson number (Ri) on the streamlines (Ψ) and isothermal (θ) for Re = 50, Pr = 7, Ri = 0.1, h = 0.6, and L_f = 0.2. From the streamlines (Ψ) in the left, it is noticed that when Ri = 0.1(weak buoyancy), there are four vortices, three of which are small, due to shear-dominated flow. The max vortex is at the fin tip, which is large in size and occupies the space before and after the fin. At Ri = 1, the primary vortex expands and is distorted above the fin. At Rayleigh (Ra) = 10, the vortex above the fin almost disappears, and the size of the central vortex increases so that it occupies half the space of the cavity, and its density also increases because of flow dominated by buoyancy force.

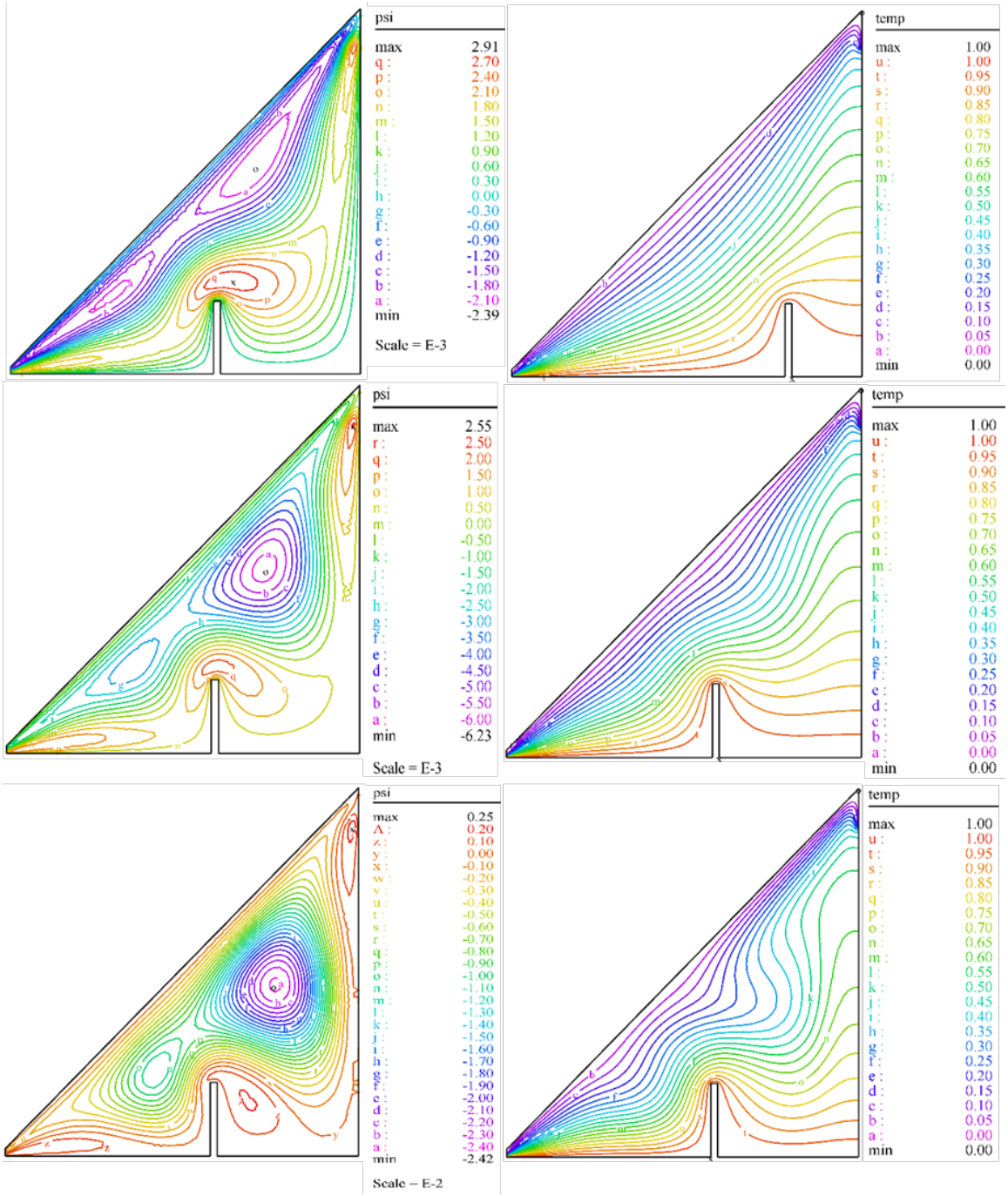

Figure 7. Streamlines (left) and isotherms (right) when L_f, h, and Re are 0.2 m, 0.6 m, and 50, respectively, and Ri equals 0.1 (upper), 1 (middle), and 10 (lower)

3.5 Re effect on Nu_{avg}

Figure 8, which represents the relationship between Nu_{avg} with Re at $L_f = 0.2$, Ri = 0.1 and h = 0.6. From the figure, we can see that Nu_{avg} depends on the Reynolds number, especially for large values of Re. When Re is low (Re < 50), the fluid flow is dominated by recirculation and viscosity forces, so $Nu_{avg} \approx 7.4$ (because driving forces dominate within the gap). The fin generates small recirculation zones and temperature gradients that do not mix significantly. In the (50–100) Re range, furthermore, thermal mixing occurs due to flow vortices increases with Re, and more convection occurs as instabilities cause Nu_{avg} to increase. As Re values become too large (Re > 100), the heat loading increases, and the fin increases turbulence in the fluid, significantly increasing the Nu_{avg}.

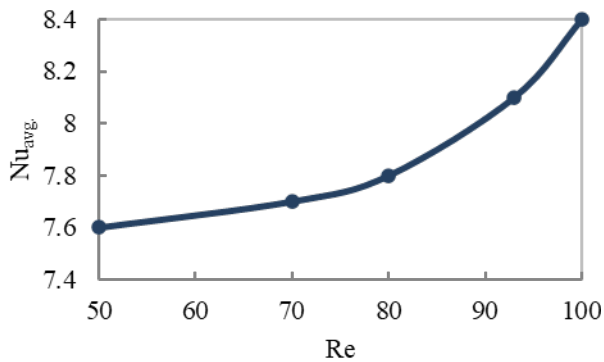

Figure 8. The relationship between Nu_{avg} and Re with L_f, Ri, and h equal 0.2, 0.1, and 0.6, respectively

3.6 The Richardson number effect on the Nusselt number

The relationship between Nu_{avg} and Ri at constants values of Re = 50, L_f = 0.2, and h = 0.6 can be shown in Figure 9. Nu_{avg} initially has a low value (e.g., Nu_{avg} = 7.6 at Ri = 0.1) due to the predominance of shear forces (i.e., weak buoyancy), but it gradually increases to approximately 8.4 at Ri = 2.1 due to mixed convection, with buoyancy-induced convection taking precedence. After this point, the value increases in a straight line with Ri until it reaches its maximum value of 9.02 at Ri = 10, since the buoyancy force increases the convection heat transfer.

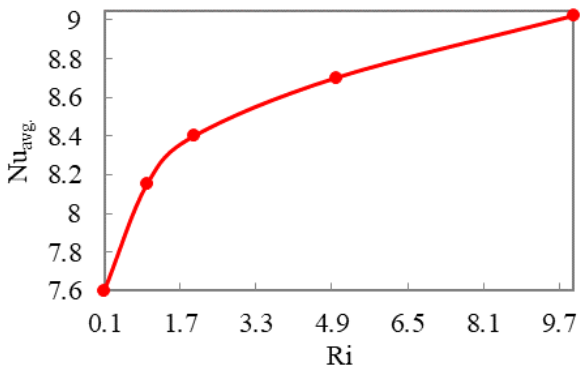

Figure 9. The relationship between Nuavg and Ri with Re, L_f, and h equal 50, 0.2, and 0.6, respectively

3.7 Fin position effect on Nusselt number

The effect of fin position on Nu can be seen in Figure 10, which draw at different values of h (0.4, 0.6, and 0.8) and constant Re = 50, L_f = 0.2 and Ri = 0.1. The curve shows how the average Nusselt number varies with the fin position on the bottom wall under laminar flow (Re = 50) and shear flow (Ri = 0.1) conditions. It is observed that $Nu_{avg.}$ increases with increasing h, since increasing h leads to flow separation, which increases the heat mixing efficiency. It can be seen that at h = 0.4, the fin has a $Nu_{avg.}$ of 7.4, while at h = 0.8, it has a peak $Nu_{avg.}$ of 8.7. The increase in Nu_{avg} is 17.6%, which is attributed to the effective convection occurring around the fin, which increases the fluid flow area. In this case, the fluid has sufficient area to accelerate around the fin, which enhances the convection and, consequently, increases Nu_{avg}.

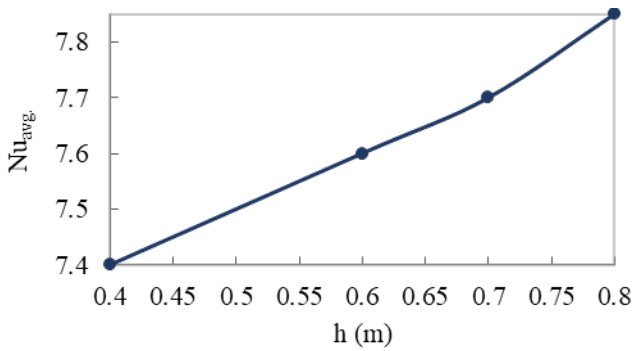

Figure 10. The relationship between Nu_{avg} and h with Re, L_f, and Ri equal 50, 0.2, and 0.1, respectively

3.8 Fin length effect on Nusselt number

Figure 11 shows the average Nu number for the L_f range (0.1 to 0.3) at Pr = 7, Re = 50, Ri = 0.1, and h = 0.6. The curve shows that $Nu_{avg.}$ decrease sharply with increasing L_f until it reaches a remarkable value of 6.65 at L_f = 0.1, then decreases linearly with increasing fin length, $Nu_{avg.}$ has a value of 6.33 at L_f = 0.3. Increasing fin length leads to poor flow recirculation and the dominance of heat conduction near the walls, which reduces convection throughout the cavity. The fin acts as a severe constraint to heat transfer, and a large stagnant region is formed behind the fin, reducing convection throughout the cavity, which reduces heat transfer and thus lowers Nu_{avg}.

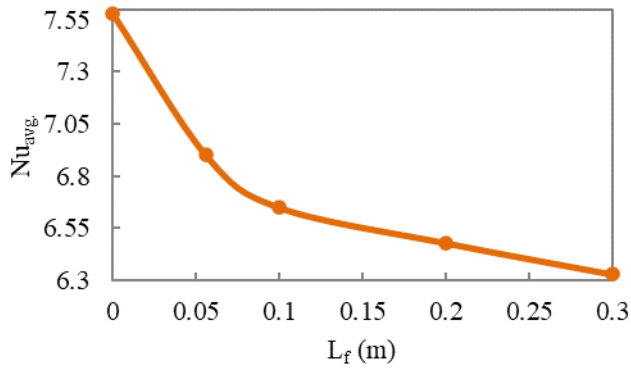

Figure 11. The relationship between Nuavg and L_f at Pr = 7 with Re, Ri, and h equal 50, 0.1, and 0.6, respectively

The flowchart for the governing equation by finite element method using the FlexPDE package can be seen in Figure 12, which appears the whole calculations process that happened in the program.

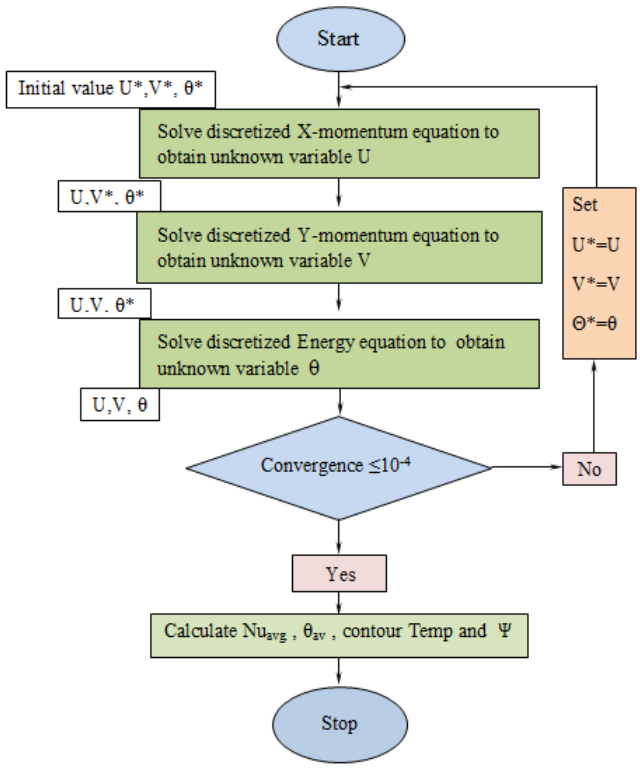

Figure 12. Flow chart of numerical solution using FlexPED package

Tables 1 and 2 appear the values of maximum psi and θ_{avg} at different values of Re number and h.

Table 1. Maximum psi for different values of Re and h

Re	h		
	0.4	0.6	0.8
	psi		
50	3.82	2.91	2.51
100	3.53	2.71	2.15
150	3.32	2.37	2.12

Table 2. Maximum θ_{avg} for different values of Re and h

Re	h		
	0.4	0.6	0.8
	θ_{avg}		
50	0.285	0.283	0.277
100	0.281	0.279	0.27
150	0.268	0.26	0.253

The results of current study make a great break according to the existing research [1, 19, 24], by providing a core reconfigurating of the relationship between a cavity and a fin. Although in the past literature, most studies are on square enclosures where passive extensions of the conductive fins are used as heat-sinks, the present findings show that a unique triangular vented cavity with an optimal arrangement of adiabatic fins is technologically superior. In contrast to the classical design which involves making the fins as large as possible, we design fin to act solely as a flow control device which is adiabatic in nature, which is used to manipulate the effective flow area in the triangular shape. The given research provides a first-of-its-kind systematic parametric mapping of fin length and placement in a mixed convection regime demonstrating how geometric blockage can be optimized to benefit thermal-hydraulic performance in a manner that was, previously, revised in literature on this particular triangular setup.

To emphasize how this work is developed in relation to the available literature, Table 3 presents a comparative overview of the presented geometric and functional innovations.

Table 3. Validation and novelty analysis: Comparative analysis of the current study against prior research

Feature / Metric	Previous Study	Current Study (Our Work)	Key Distinction
Cavity Geometry	1. Al-Farhany et al. [10, 11]: Often rectangular or simple square cavities, varied (Square enclosure with inclined baffle, Nanofluids). 2. Selimefendigil and Chamkha [16]: Often rectangular or simple square cavities, varied (3D vented cavity with inner rotating cylinder, MHD). 3. Çiçek and Baytaş [19]: Square / Various (Systematic Review). 4. Al-Maliki et al. [12]: Vented Square Cavity. Abu Ghurban et al. [24]: Triangular Enclosure (Natural Convection focus).	Distinctive and adiabatic triangular vented cavity geometry	Novel geometry explored
Fin Application	1. Al-Farhany et al. [10, 11]: Usually adiabatic (conducts heat) fins for heat transfer enhancement. 2. Selimefendigil and Chamkha [16]: Usually adiabatic (conducts heat) fins for heat transfer enhancement. 3. Çiçek and Baytaş [19]: Primarily Adiabatic / Solid obstacles. 4. Al-Maliki et al. [12]: Conductive (Aluminum) Fin. Abu Ghurban et al. [24]: No Fin / Internal circular cylinder.	Adiabatic fin on the hot wall	Focus on flow control, not heat transfer area
Fin Purpose	1. Al-Farhany et al. [10, 11]: Primary use: increase heat transfer surface area (Effect of baffle angle and Nanofluid on natural convection). 2. Selimefendigil and Chamkha [16]: Primary use is increasing heat transfer surface area (MHD effects on mixed convection with active rotating element). 3. Çiçek and Baytaş [19]: Heat transfer enhancement using surface area (Entropy generation in mixed convection with particles). 4. Al-Maliki et al. [12]: Heat transfer enhancement via conduction (Experimental study of hybrid Nanofluid with PCM for temperature damping). Abu Ghurban et al. [24]: Numerical study of fin effect on mixed convection.	Primary use: flow control technique to increase effective flow area	Functional novelty
Parametric Study	1. Al-Farhany et al. [10, 11]: Limited to certain aspects like fin size or placement in simple shapes. 2. Selimefendigil and Chamkha [16]: Limited to certain aspects like fin size or placement in simple shapes. 3. Çiçek and Baytaş [19]: Shape optimization & Nanofluid effects. 4. Al-Maliki et al. [12]: Fin length & location impact on Nu_{avg} cap. Abu Ghurban et al. [24]: Rotation angle and aspect ratio.	Systematic study of positioning and length of fins in a mixed convection regime	Comprehensive parameter analysis in a unique setup
Convection	1. Al-Farhany et al. [10, 11]: Various regimes	Mixed convection regime	Specific regime for this

Regime	studied. 2. Selimefendigil and Chamkha [16]: Various regimes studied. 3. Çiçek and Baytaş [19]: Natural / Various. 4. Al-Maliki et al. [12]: Mixed Convection. Abu Ghurban et al. [24]: Natural Convection.		unique setup
Novelty Status/Limitations	1. Al-Farhany et al. [10, 11]: Established research in general cavity flow/ Focusing on natural convection (Ri < 0.1) in sealed enclosures. Does not address mixed convection in vented configurations or the role of adiabatic flow-modifying structures. 2. Selimefendigil and Chamkha [16]: Established research in general cavity flow. 3. Çiçek and Baytaş [19]: Established configuration review/ Focusing on second-law analysis with particulate flow. The geometric effect of a triangular cavity with a strategically placed adiabatic fin on first-law performance (Nu) is not covered. 4. Al-Maliki et al. [12]: Investigating thermal energy storage using standard vented geometry/ Release via PCM (does not explore the fluid-dynamic mechanism of expanding the effective flow area using a simple adiabatic obstruction). 5. Abu Ghurban et al. [24]: Closed triangular geometry/Their triangular cavities geometry does not introduces asymmetric flow paths and distinct vortex interactions between the slanted adiabatic wall and the fin.	First-ever revision in literature for this specific application/geometry	Overall uniqueness (Never before revised in literature for this configuration)

3.9 Limitations and contextualization

Although the current study offers some meaningful information on the enhancement of the mixed convection through the use of an adiabatic fin in a triangular vented cavity, it is important to note that there are a number of limitations that can be identified to effectively contextualize the results of the study and inform future research. The current analysis is done in laminar flow conditions with the working fluid being water (Pr = 7) at laminar flow. This option will allow easy comparison to basic research but restrict the direct applicability to other systems that use either air (Pr ≈ 0.7) or Nanofluid with variable properties. As an example, there is a research showed that the application of Al_2O_3 water nanofluids in a radiator had the potential to change the pressure drop and heat transfer behavior by modifying the effective viscosity and thermal conductivity [14]. The model we use does not take into consideration such variations of property or particle. Also, dynamics, which might adjust the optimal fin position and the reported trends of Nusselt number. Moreover, the study is limited to a 2D steady-state model. Although this simplification is typical of preliminary parametric investigations three-dimensional flow interaction, temporary heating, and turbulent systems (Re > 150) are typical of real-world scenarios [13]. In one case, another research demonstrated that 3D cavity simulations (rotating cylinders) have a strong variation in vortex structures and heat transfer [16]. We might thus be over predicting the 2D coincidence of re circulation areas and underestimating the complexity of flow detachment and reattachment during a flow around the fin in a realistic, 3D environment. Also, the fin has been simplified as a perfect adiabatic case, a theoretical extreme that isolates the flow-modifying effects of the fin.

Practically, even bad conductive materials are heat conductors. Another papers investigated conductive baffles in nanofluids-filled enclosures and have discovered that conductive fins actively engage in the heat redistribution process, modifying local isotherms, and total thermal resistance [10, 11]. The applicability of our results on fin placement and length would be best in applications where the main objective of the fin is to control flow not heat transfer e.g. polymer flow guides or insulated baffles in a ventilation system. Additionally, the ranges of Re (50–150) and Ri (0.1–10) studied are devoted to the laminar mixed convection with a moderate strength of the buoyancy forces. The linear dependence of Nu_{avg} on Ri (Figure 9) may not be valid in a strongly forced (Ri << 0.1) or strongly buoyant (Ri >> 10) regime in which the dynamics change dramatically. Moreover, although our analysis establishes an optimal value of h (0.8) where the given configuration has a minimum pressure drop, this minimum is probably finely dependent on the aspect ratio of the cavity, the location of the inlet and outlet, and the Prandtl number of the working fluid as predicted by parametric sensitivities in comparable experiments on vented enclosures [19, 24].

In addition, the numerical validation was also conducted as compared to benchmark cases and grid independence studies and this ensures reliability of the solutions under the assumed model. There, however, is no experimental corroboration. The usefulness of empirical validation of our ideal numerical model is seen in studies [12], who have coupled experimental and numerical methods to hybrid Nanofluid-PCM systems, which takes into account the reality of surface roughness, minor geometrical imperfections, and unsteady effects. Finally, the fact that shorter fins (L_f = 0.1) are better at heat transfer than longer ones is in line with the overall rule of too much flow obstruction being harmful, which is also observed in baffle experiments [10, 24]. But the extent of the improvement (e.g., 17.6 percent increase in Nu_{avg} with optimal fin placement) is geometry-dependent and adiabatic. Conversely, conductive fin or baffle research into square cavities does not find the same optimal dimensions and percentage of improvement and highlights the geometry-sensitive nature of thermal optimization [24].

4. CONCLUSIONS

This study evaluated the impact of geometric and dimensionless parameters on the thermal performance of a 2D triangular vented cavity, demonstrating that the thermal performance of a 2D triangular vented cavity is primarily governed by the strategic integration of an adiabatic fin and the modulation of dimensionless parameters. The results establish that fin placement is a critical mechanism for managing recirculation intensity and isothermal patterns, with centrally located fins offering precise control for specialized thermal applications. Furthermore, the Richardson number (Ri) was identified as the dominant design criterion, as its variation radically shifts the flow physics and directly determines the average Nusselt number (Nu_{avg}). While heat transfer transitions from diffusion-dominated to convection-dominated regimes with increasing Reynolds number (Re), the efficiency does not scale linearly with geometry; instead, shorter fins optimize (Nu_{avg}) by facilitating mass convection, whereas longer fins impede thermal performance by obstructing flow. Ultimately, the fin position (h) serves as a foundational optimization parameter that significantly modulates heat transfer rates even under constant flow conditions.

By demonstrating that the interaction of a triangular geometry of a vented cavity and an adiabatic fin on the heated wall constitutes a significant influence on the management of flows and heat transfer properties, our study would also add a new dimension to mixed convective heat transfer. Moreover, we reveal that a systematic parametric study of fin placement and length in this particular mixed convection regime can present new information about the expansion of the area of effective flow, which has not been experimented with and documented in the literature so far.

Several other questions remain to be addressed, such as extending the model to three dimensions and include turbulent flow regimes, investigating the effects of nanofluids or hybrid coolants with temperature-dependent properties, considering flexible or actively controlled fins to adapt to varying thermal loads, as preliminarily explored in fluid-structure interaction studies, and performing experimental validation using scaled models or representative electronic cooling setups to verify the numerical predictions under realistic conditions. Furthermore, investigations can be done on effects of non-Newtonian fluids or 3D effects so as to optimize the fin-based thermal management system further.

REFERENCES

[1] Xuan, Y., Roetzel, W. (2000). Conceptions for heat transfer correlation of nanofluids. International Journal of Heat and Mass Transfer, 43(19): 3701-3707. https://doi.org/10.1016/s0017-9310(99)00369-5

[2] Purusothaman, A. (2018), Investigation of natural convection heat transfer performance of the QFN-PCB electronic module by using nanofluid for power electronics cooling applications. Advanced Powder Technology, 29(4): 996-1004. https://doi.org/10.1016/j.apt.2018.01.018

[3] Baïri, A., Laraqi, N. (2019). Experimental quantification of natural convective heat transfer within annulus space filled with a H_2O-Cu nanofluid saturated porous medium. Application to electronics cooling. Experimental Heat Transfer, 32(4): 364-375. https://doi.org/10.1080/08916152.2018.1526230

[4] Chen, G., Tang, Y., Wan, Z., Zhong, G., Tang, H., Zeng J. (2019). Heat transfer characteristic of an ultra-thin flat plate heat pipe with surface-functional wicks for cooling electronics. International Communications in Heat and Mass Transfer, 100(1): 12-19. https://doi.org/10.1016/j.icheatmasstransfer.2018.10.011

[5] Hiba, B., Redouane, F., Jamshed, W., Ahamed C., Saleel, S., Suriya, U.D., Prakash, M., Nisar, K.S., Vijayakumar, V., Eid, M.R. (2021). A novel case study ofthermal and streamline analysis in a grooved enclosure filled with (Ag–MgO/Water) hybrid nanofluid: Galerkin FEM. Case Studies in Thermal Engineering, 28(1): 101372. https://doi.org/10.1016/j.csite.2021.101372

[6] Ahmadi, A., Ehyaei, M.A., Doustgani, A., El Haj Assad, M., Hmida, A., Jamali, D.H., Kumar, R., Li, Z.X., Razmjoo, A. (2021). Recent residential applications of low-temperature solar collector. Journal of Cleaner Production, 279(1): 123549. https://doi.org/10.1016/j.jclepro.2020.123549

[7] Liu, W., Bie, Y., Xu, T., Cichon, A., Królczyk, G., Li, Z. (2022). Heat transfer enhancement of latent heat thermal energy storage in solar heating system: A state-of-the-art review. Journal of Energy Storage, 46(1): 103727. https://doi.org/10.1016/j.est.2021.103727

[8] Sirikasemsuk, S., Wiriyasart, S., Prurapark, R., Naphon, N., Naphon, P. (2021). Water/nanofluid pulsating flow inthermoelectric module for cooling electric vehicle battery systems. International Journal of Heat and Technology, 39(5): 1618-1626. https://doi.org/10.18280/ijht.390525

[9] Rashidi, M.M., Mahariq, I., Alhuyi Nazari, M., Accouche, O., Bhatti, M.M. (2022). Comprehensive review on exergy analysis of shell and tube heat exchangers. Journal of Thermal Analysis and Calorimetry, 147(22): 12301-12311. https://doi.org/10.1007/s10973-022-11478-2

[10] Al-Farhany, K., Al-Muhja, B., Karuppusamy, L., Periyasamy, U., Ali, F., Sarris, I. (2022). Analysis of convection phenomenon in enclosure utilizing nanofluids with baffle effects. Energies, 15: 6615. https://doi.org/10.3390/en15186615

[11] Al-Farhany, K., Al Muhja, B., Ali, F., Khan, U., Zaib, A., Raizah, Z., Galal, A.M. (2022). The baffle length effects on the natural convection in nanofluid filled square enclosure with sinusoidal temperature. Molecules, 27(14): 4445. https://doi.org/10.3390/molecules27144445

[12] Al-Maliki, M., Al-Farhany, K., Sarris, I.E. (2022). Heat transfer in an inclined rectangular cavity filled with hybrid nanofluid attached to a vertical heated wall integrated with PCM: An experimental study. Symmetry, 14(10): 2181. https://doi.org/10.3390/sym14102181

[13] Al-Farhany, K., Al-dawody, M.F., Hamzah, D.A., Al-Kouz, W., Said, Z. (2023). Numerical investigation of natural convection on Al_2O_3–water porous enclosure partially heated with two fins attached to its hot wall: Under the MHD effects. Applied Nanoscience, 13(14): 555-572. https://doi.org/10.1007/s13204-021-01855-y

[14] Canazas, J., Kamyshnikov, O. (2022). Heat transfer and pressure drop performance of a hydraulic mining shovel radiator by using ethylene glycol/water-based Al2O3

nanofluids. International Journal of Heat and Technology, 40(1): 273-281. https://doi.org/10.18280/ijht.400132
[15] Velkennedy, R., Jeseema Nisrin, J., Kalidasan, K., Rajeshkanna, P. (2021). Numerical investigation of convective heat transfer in a rectangular vented cavity with two outlets and cold partitions. International Communications in Heat and Mass Transfer, 129(1): 105659. https://doi.org/10.1016/j.icheatmasstransfer.2021.105659
[16] Selimefendigil, F., Chamkha, A.J. (2020). MHD mixed convection of nanofluid in a three-dimensional vented cavity with surface corrugation and inner rotating cylinder. International Journal of Numerical Methods for Heat & Fluid Flow, 30(4): 1637-1660. https://doi.org/10.1108/HFF-10-2018-0566
[17] Alhussain, Z.A. (2022). Mixed convective flow in a multiple port ventilation square cavity with insulated baffle. Case Studies in Thermal Engineering, 30(1): 101785. https://doi.org/10.1016/j.csite.2022.101785
[18] Shaker, H., Abbasalizadeh, M., Khalilarya, S., Motlagh, S.Y. (2021). Two-phase modeling of the effect of non-uniform magnetic field on mixed convection of magnetic nanofluids inside an opencavity. International Journal of Mechanical Sciences, 207(1): 106666. https://doi.org/10.1016/j.ijmecsci.2021.106666
[19] Çiçek, O., Baytaş, A.C. (2023). A numerical investigation of the particle behaviors and entropy generation in mixed convection inside a vented enclosure. International Journal of Thermal Sciences, 185(1): 108058. https://doi.org/10.1016/j.ijthermalsci.2022.108058
[20] Angirasa, D. (2000). Mixed convection in a vented enclosure with an isothermal vertical surface, Fluid Dynamics Research, 26(4): 219-233. https://doi.org/10.1016/S0169-5983(99)00024-6
[21] Ismael, M.A., Jasim, H.F. (2018). Role of the fluid-structure interaction in mixed convection in a vented cavity. International Journal of Mechanical Sciences, 135: 190-202. https://doi.org/10.1016/j.ijmecsci.2017.11.001
[22] Saleh, H., Naganthran, K., Hashim, I., Ghalambaz, M., Nazar, R. (2022). Role of fluid-structure interaction in free convection in square open cavity with double flexible oscillating fins. Alexandria Engineering Journal, 61(2): 1217-1234. https://doi.org/10.1016/j.aej.2021.04.073
[23] Shahabadi, M., Mehryan, S.A.M., Ghalambaz, M., Ismael, M. (2021). Controlling the natural convection of a non-Newtonian fluid using a flexible fin. Applied Mathematical Modelling, 92: 669-686. https://doi.org/10.1016/j.apm.2020.11.029
[24] Abu Ghurban M., AlFarhany, K., Kada, B. (2023). Effects of fin on mixed convection heat transfer in a vented square cavity: A numerical study. Al-Qadisiyah Journal for Engineering Sciences, 16: 200-208. https://doi.org/10.30772/qjes.2023.142305.1016
[25] Purusothaman, A. (2018). Investigation of natural convection heat transfer performance of the QFN-PCB electronic module by using nanofluid for power electronics cooling applications. Advanced Powder Technology, 29(4): 996-1004. https://doi.org/10.1016/j.apt.2018.01.018
[26] Alshara, A.K., Abood, F.A., Al-mayahi, H.A. (2013). Mixed convection heat transfer inside a vented square enclosure with concentric rotation inner cylinder. Thi-Qar University Journal for Engineering Sciences, 4(3): 60-76. https://doi.org/10.31663/utjes.v4i3.187
[27] Sivasankaran, S., Janagi, K. (2022). Numerical study on mixed convection flow and energy transfer in an inclined channel cavity: Effect of baffle size. Mathematical and Computational Applications, 27(1): 9. https://doi.org/10.3390/mca27010009
[28] Yaseen, S.J. (2023). Numerical study of the fluid flow and heat transfer in a finned heat sink using Ansys Icepak. Open Engineering, 13(1): 20220440. https://doi.org/10.1515/eng-2022-0440
[29] Backstrom, G. (2005). Field of physics by finite element analysis using FlexPDE. GB Publishing, Malmö, Sweedn.
[30] Oyewola, O.M., Afolabi, S., Ismail, O.S. (2021). Numerical simulation of natural convection in rectangular cavities with different aspect ratios. Frontiers in Heat and Mass Transfer (FHMT), 17(11): 1-8. https://doi.org/10.5098/hmt.17.11
[31] Mutasher, D.G. (2024). Advances in oscillating fin technologies for heat transfer enhancement: A review of numerical and experimental approaches. Power Engineering and Engineering Thermophysics, 3(4): 279-297. https://doi.org/10.56578/peet030405
[32] Alshara, A.K.M. (2012). Effect of single or multi rotating horizntal cylinder on the mixed convection heat transfer inside a triangular enclosure. Al-Qadisiya Journal for Engineering Sciences, 5(1): 95-110.
[33] Batista, R.C., Rajendran, R.C. (2023). Computational analysis of thermal performance augmentation in helical coil heat exchangers via CuO/water nanofluid. Power Engineering and Engineering Thermophysics, 2(3): 139-149. https://doi.org/10.56578/peet020302
[34] Roy, S., Basak, T. (2005), Finite element analysis of natural convection flows in square cavity with non-uniformly heated wall(s). International Journal of Engineering and Science, 43: 668-680. https://doi.org/10.1016/j.ijengsci.2005.01.002

NOMENCLATURE

CP	specific heat, $J \cdot kg^{-1} \cdot K^{-1}$
g	gravitational acceleration, $m \cdot s^{-2}$
h	fin position
k	thermal conductivity, $W \cdot m^{-1} \cdot K^{-1}$
L	length of the cavity
L_f	length of the fin
Nu	local Nusselt number along the heat source
Nu_{avg}	average Nusselt number
P	pressure
Pr	Prandtl number
psi	stream function
Ra	Rayleigh number
Re	Reynolds number
Ri	Richardson number
T	dimensional temperature
U, V	dimensionless velocity components
W	sizes of inlet and outlet holes
X, Y	dimensionless coordinates

Greek symbols

β	thermal expansion coefficient
$\theta_{avg.}$	dimensionless bulk temperature
θ	dimensionless temperature
ν	kinematic viscosity
Ψ	streamlines
ρ	density

Subscripts

avg	average
c	cold temperature
f	fin
h	hot temperature
in	inlet
out	outlet